Off-the-shelf diodes as high-voltage opening switches

Off-the-Shelf Diodes as High-Voltage Opening Switches

Mawuena Rémi Degnon, *Graduate Student Member, IEEE*, Anton I. Gusev, *Member, IEEE*, Antoine Silvestre de Ferron, Laurent Pécastaing, *Senior Member, IEEE*, Gaëtan Daulhac, Aleksandr Baranov, Sébastien Boisne, and Bucur Mircea Novac, *Senior Member, IEEE*

***Abstract*— A semiconductor opening switch (SOS) (also known as SOS diode) is a solid-state nanosecond switch of gigawatt power level. Due to its high pulse repetition rate, long lifetime, and maintenance-free capability, the SOS diodes are becoming increasingly attractive for use in solid-state pulsed power generators. However, the lack of SOS diode manufacturers prevents the widespread use of this technology. This work demonstrates the ability of off-the-shelf diodes to operate in the SOS mode. A wide range of off-the-shelf diodes including rectifier, fast recovery, avalanche, and transient-voltage-suppression (TVS) diodes have been tested as high-voltage opening switches. An experimental arrangement based on a saturating pulse transformer (PT) was developed to test off-the-shelf diodes in the SOS mode. The results obtained were compared with the existent top of the range SOS diodes, used as reference. Two versions of the experimental setup with the initially stored energy of 25 mJ and 10 J were used. The following pulse parameters were obtained using off-the-shelf diodes: 1) peak voltage impulse of 3 kV and rise time of 10 ns with a 110 Ω load (for the 25 mJ setup) and 2) peak voltage impulse of 80 kV and rise time of 20 ns with a 1 kΩ load (for the 10 J setup). Based on the parameters obtained, the door is opened for a future use of off-the-shelf diodes as opening switches in a wide range of solid-state-based pulsed power systems.**

***Index Terms*— Off-the-shelf diode, pulsed power system, saturating pulse transformer (PT), semiconductor opening switch (SOS).**

Manuscript received February 1, 2022; revised April 8, 2022; accepted May 14, 2022. This work was supported in part by the French "Investissements d'Avenir" Program within the Framework of the Energy and Environment Solutions-Université de Pau et des Pays de l'Adour (E2S UPPA) Project [Solid-State Pulsed Power (S2P2) and Pulsed Power Applications (PULPA) Chairs] managed by the Agence Nationale de la Recherche (ANR) under Grant ANR-16-IDEX-0002 and in part by ITHPP ALCEN. The review of this article was arranged by Senior Editor R. P. Joshi. *(Corresponding author: Mawuena Rémi Degnon.)*

Mawuena Rémi Degnon is with the SIAME Laboratory, E2S UPPA, Université de Pau et des Pays de l'Adour, 64000 Pau, France, and also with ITHPP ALCEN, 46500 Thégra, France (e-mail: rdegnon@ithpp-alcen.fr).

Anton I. Gusev, Antoine Silvestre de Ferron, and Laurent Pécastaing are with the SIAME Laboratory, E2S UPPA, Université de Pau et des Pays de l'Adour, 64000 Pau, France (e-mail: anton.gusev@univ-pau.fr).

Gaëtan Daulhac, Aleksandr Baranov, and Sébastien Boisne are with ITHPP ALCEN, 46500 Thégra, France (e-mail: sboisne@ithpp-alcen.fr).

Bucur Mircea Novac is with the Wolfson School of Mechanical, Electrical and Manufacturing Engineering, Loughborough University, Loughborough LE11 3TU, U.K., and also with the SIAME Laboratory, E2S UPPA, Université de Pau et des Pays de l'Adour, 64000 Pau, France (e-mail: b.m.novac@lboro.ac.uk).

Color versions of one or more figures in this article are available at https://doi.org/10.1109/TPS.2022.3177702.

Digital Object Identifier 10.1109/TPS.2022.3177702

I. Introduction

THE switch is one of the fundamental components of all pulsed power system and can be either a closing or an opening type. The type of switch used depends on the way the energy is stored. Closing switches are used in capacitive (electric) energy storage (CES) systems, such as Marx generators and pulse forming lines. Opening switches are used in circuits based on inductive (magnetic) energy storage (IES), which have a higher energy density than CES [1]. According to [2], there are several fundamental differences between these two types of switches, which put the opening switch in a more attractive position for nanosecond pulsed power technology. An opening switch allows faster energy transfer, with the current cutting-off process increasing the output voltage, which results in a pulsed power gain.

However, while it is simpler to switch the energy stored in CES through conventional spark gap closing switches, the requirements on opening switches used in IES are usually challenging, particularly when it is required to switch-off, rapidly and repetitively, several kAs to generate hundreds of kVs or even a few megavolts (MVs) pulses [3]. Solid-state devices are widely used in power electronics, such as the insulated-gate bipolar transistor (IGBT), the gate turn-off thyristor (GTO), and the metal–oxide–semiconductor field-effect transistor (MOSFET). All these are potentially usable as opening switches; however, they are currently limited either by a maximum current or by their switching characteristic speed [4]–[6]. With some very few exceptions, the plasma opening switch or the exploding wire is unsuitable for high pulsed repetition frequency (PRF) operation and has a limited lifetime [1], [2].

Toward the end of the 20th century, the semiconductor opening switch (SOS) effect was discovered in $p^+ - p - n - n^+$ silicon diode structure by Mesyats *et al.* [7]. The SOS effect is the nanosecond cutoff of high-density reverse currents in semiconductor diodes, for which a theoretical model was proposed in [8]. Based on this effect, SOS diodes were developed over three decades ago [9]. That sparked a breakthrough in the development of solid-state pulsed power systems based on IES, since it allows the improvement of their important characteristics such as current density, pulsed power, voltage, energy, and PRF [10], [11]. Due to high PRF of operation, long lifetime, and high average power, the SOS generators are currently used not only in research but also in

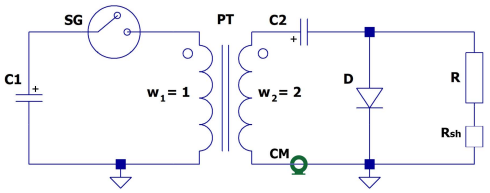

Fig. 1. Circuit diagram of the 25 mJ experimental arrangement. Explanations are provided in the text.

modern biological, medical, and industrial applications, such as X-ray pulsed sources, particle accelerators, non-thermal plasma purification of water and gas, e-beam sterilization, laser pumping sources, and many other [12]–[18].

However, the interest in the benefits of SOS for improving the performance of pulsed power systems sharply contrasts with a lack of SOS diode manufacturers. Hence, demonstrating the possibility of using off-the-shelf diodes as SOS diodes represents the main aim of the research presented in this article. A wide range of off-the-shelf diodes have been tested as high-voltage opening switches at switching energies of up to 10 J. The results are presented in Sections II and III, respectively, devoted to the 25 mJ and 10 J experimental arrangements. Section IV is devoted to conclusions.

II. 25 mJ Experimental Arrangement

A. Circuit Description

A simplified circuit of the low-energy test bench is shown in Fig. 1. The circuit is designed with a single magnetic element to ensure high energy efficiency, which can be up to 70% [19]. For convenience, a self-breakdown spark gap (SG) is used as a primary switch. The ceramic capacitors $C1$ and $C2$ have a capacitance of 50 and 12.5 nF, respectively. The magnetic core of the pulse transformer (PT) consists of a single nanocrystalline ring (110 mm × 80 mm × 20 mm) obtained from Vacuumschmelze, with the saturation induction being 1.2 T [20]. The saturating magnetic core PT ensures two main functions. The first is to transfer the energy from the primary to the secondary circuit, stepping up the voltage. The second is to have a very low inductance of the secondary winding, when the magnetic core is driven to saturation. The primary and secondary windings of PT have $w_1 = 1$ and $w_2 = 2$ turns, respectively. A bias winding of two turns (not shown) with a maximum current amplitude of 3 A is used to reset the core before the next pulse. The low-inductance resistive load R is connected in parallel to the diode D under test.

The circuit of Fig. 1 operates as follows. First, $C1$ is charged to its initial voltage V_C1 by an external dc power supply (not shown). When SG closes, $C1$ releases its energy and the PT charges $C2$, while the current flows through the diode D in the forward direction. For an SOS diode, this is the forward pumping stage, which lasts for t^+ while the current reaches its maximum amplitude I^+ [see Fig. 2(a)]. The circuit is designed using the voltage–time product [21] to reach the maximum voltage across $C2$ at the moment when the magnetic core of the PT saturates. At this moment, $C2$ starts to discharge through the secondary winding w_2 of the saturated PT, generating the reverse current through the diode. This represents the reverse pumping stage for the SOS diode, where

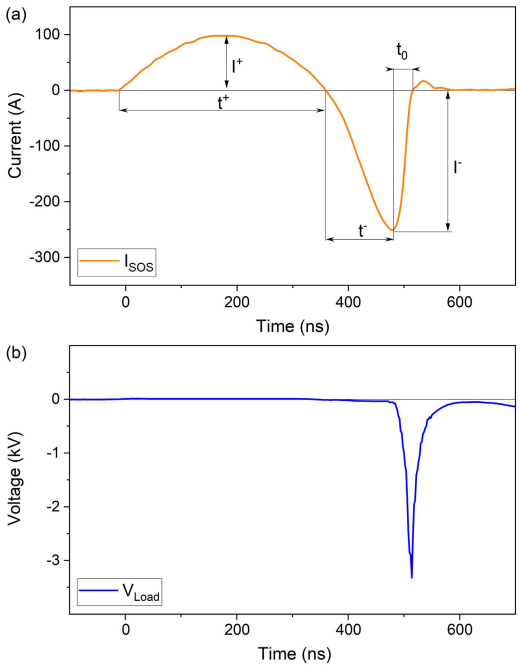

Fig. 2. Typical waveforms of the current flowing through (a) SOS-R diode and (b) voltage across the load $R = 28\ \Omega$ for $V_C1 = 1$ kV.

the current reaches the maximum amplitude I^- after a duration t^- [see Fig. 2(a)]. The magnitude of the reverse current, and thus the reverse current density, is greater than the forward current due to the much lower self-inductance of the saturated PT. Finally, this reverse current is cut off within the switching time t_0 [see Fig.2(a)] by the SOS diode and the energy is transferred to the load R, generating a very short nanosecond high-voltage pulse with a characteristic rise time Tr [see Fig. 2(b)].

A reverse current with a density of more than 1 kA/cm^2 leads to a high electric field region, which is formed in the p region of the SOS diode structure ($p^+ - p - n - n^+$) due to the electron–hole plasma motion. Hence, in the SOS diode, the current interruption occurs in the p region rather than in the p-n-junction. Details of the SOS diode physics are described in [2].

All rise times in the present article are defined as the time interval from 10% to 90% of the peak impulse. The charging voltage of $C1$ is measured using the Tektronix probe P6015A. The voltage across the load and the current through the diodes are obtained using the current measurements of the Pearson current monitor (CM in Fig. 1) model 410 and the resistive shunt Rsh = 0.9 Ω (see Fig. 1). The waveforms are captured using Rigol DS1204B real-time oscilloscope.

B. Low-Voltage Diodes

A total of 25 types of off-the-shelf diodes were selected and tested as opening switches including rectifying, avalanche, Schottky, transient voltage suppression (TVS), and Zener diodes. The specifications of the studied diodes are as follows: blocking voltage ranging from 0.2 to 10 kV, die area from 0.01 to 0.81 cm^2 and a recovery time from 0.1 to 20 μs. The die area of each diode was measured to calculate the cutting current density which, according to [7], must be more

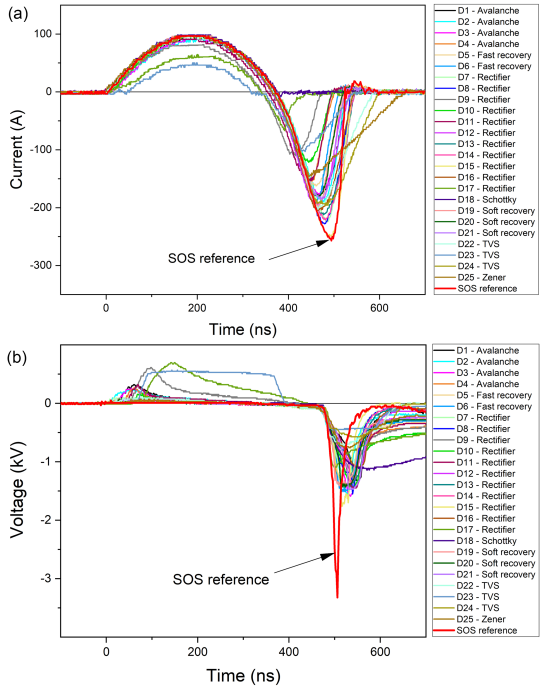

Fig. 3. (a) Current and (b) voltage waveforms of the tested off-the-shelf diodes in comparison to the SOS reference diode.

than 1 kA/cm^2 in the SOS mode of operation. SOS diodes manufactured in Russia and kindly provided by the Institute of Electrophysics, having 0.25 cm^2 die area and 3 kV rated voltage, and here termed SOS-R, are used as a reference to which the characteristics of all the off-the-shelf units are compared to.

C. Results and Discussion

First, the reference SOS-R diode is tested in the circuit shown in Fig. 1 with the charging voltage V_C1 fixed at 1 kV. The results obtained using SOS-R with a load resistance $R = 28\ \Omega$ are presented in Fig. 2. A forward pumping current $I^+ = 100$ A flows through the single SOS diode within $t^+ = 380$ ns. After saturation of the magnetic core of the PT, a reverse current $I^- = 260$ A flows through the diode for a duration $t^- = 120$ ns. After that, the current is cut off by the SOS-R diode within a time $t_0 = 34$ ns. A voltage pulse with an amplitude of 3.4 kV and a rise time of 20 ns is obtained at the load. The voltage amplitude V_C2 measured at the capacitor $C2$ is 1.7 kV, which gives an SOS-R overvoltage coefficient of 2, which is defined as $K_{ov} = V_R/V_C2$.

Second, after testing the SOS-R, all the 25 selected off-the-shelf diodes were tested one by one, in the same configuration as the SOS-R diode. Fig. 3 shows all the current and voltage waveforms obtained during these tests in comparison to the results obtained from the SOS-R diode.

As a general observation, it is clear that not all diodes can operate in the SOS mode. Rectifier, avalanche, Zener, and TVS diodes are able to open and transfer the current to the load. However, the switching time greatly varies. At the same time, the Schottky diodes, due to their structure and physics of operation, are not capable of reaching and interrupting the high reverse current. Small-area high-voltage diodes demonstrate a voltage drop during the forward current, which leads to additional energy losses and reduces the efficiency of the switch. Also, for most of the tested off-the-shelf diodes, the output voltage was limited to the level of the rated voltage for a switch consisting of a single diode.

TABLE I

VOLTAGE PULSE PARAMETERS OF THE BEST TESTED OFF-THE-SHELF OPENING SWITCHES AT $V_C1 = 1$ KV AND $R = 28\ \Omega$

Diode type	Connections		V_R	T_r (ns)	FWHM
	Series	Parallel	(kV)	(10-90%)	(ns)
Rectifier	2	2	1.85	21.2	40
Avalanche	2	20	1.96	22.4	38
Fast recovery	2	1	2.54	27.1	28
TVS	7	3	1.83	13.2	45
SOS (Ref.)	1	1	3.35	19.5	16

To overcome the voltage limitation and to reduce the voltage drop during the forward current, a series–parallel connection of the diodes has also been studied. The parallel connection aims at reducing the voltage drop, while the series connection increases the blocking voltage capability. The even distribution of voltage across the series-connected SOS diodes [22] makes it possible to assemble the diodes without any voltage distribution circuit consideration. The best results obtained from different types of single diodes are shown in Fig. 4(a); the improvement of the series–parallel connections can be seen in Fig. 4(b). The voltage capability of the off-the-shelf diodes is thus improved and, as a result, nanosecond voltages ranging from 1.8 to 2.5 kV were obtained on the resistive load of 28 Ω instead of 0.5 to 1.4 kV for single diodes. However, the highest corresponding overvoltage coefficient of the off-the-shelf diodes is 1.5, which is less than the coefficient obtained for the reference SOS-R diode that equals 2.

Even though the off-the-shelf diodes produce pulses with a voltage amplitude of about 25% less than the SOS diode, the obtained results confirm the possibility of using the off-the-shelf diodes as opening switches for IES circuits at the low energy level of 25 mJ. From a summary of the relevant parameters presented in Table I, one can see that the TVS diodes, in particular, have the fastest switching time of 13 ns compared with the other types of tested diodes. In addition, the full width at half maximum (FWHM) of the off-the-shelf diodes' voltages are 1.6–3 times longer than the SOS-R.

Furthermore, a 3.15 kV output voltage with a rise time of 10 ns and an FWHM of 40 ns was obtained on a 110 Ω load using an assembly of 64 (8 series × 8 parallel) TVS diodes at a charging voltage across $C1$ of $V_C1 = 1.9$ kV (see Fig. 5). In this configuration, the forward current of duration $t^+ = 360$ ns reached an amplitude I^+ of 170 A, while the reverse current after flowing for $t^- = 100$ ns reached the amplitude I^- of 375 A with the diode having a current cutoff time of 30 ns.

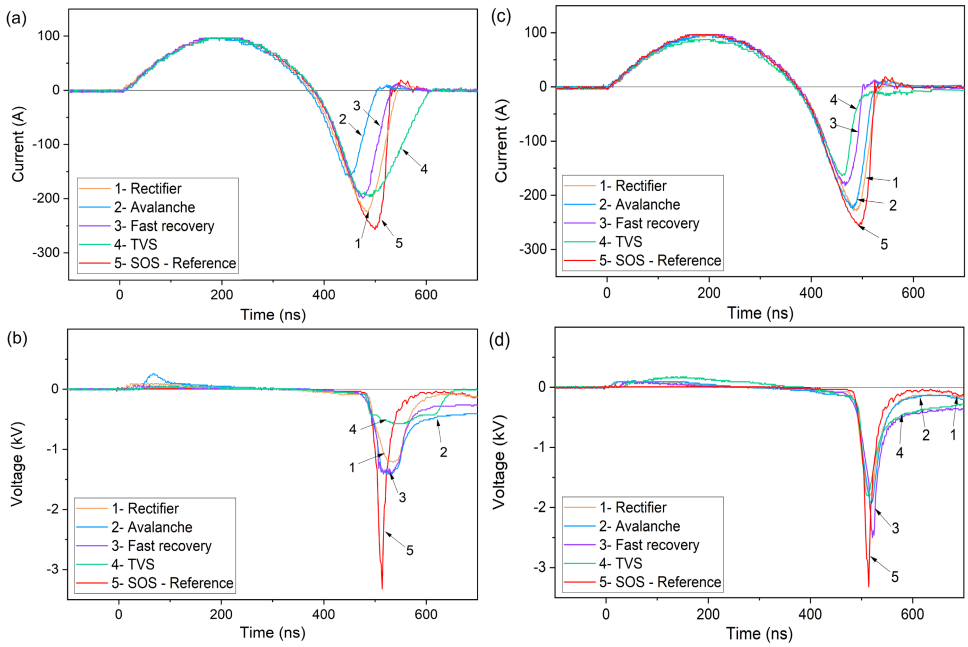

Fig. 4. Current and voltage curves of the best pulse of each type of (a) and (b) single diode and (c) and (d) diodes connected in series–parallel (1—Rectifier: 2 series × 2 parallels, 2—Avalanche: 2 series × 20 parallels, 3—Fast recovery: 2 series, and 4—TVS: 7 series × 3 parallels) at the load of 28 Ω.

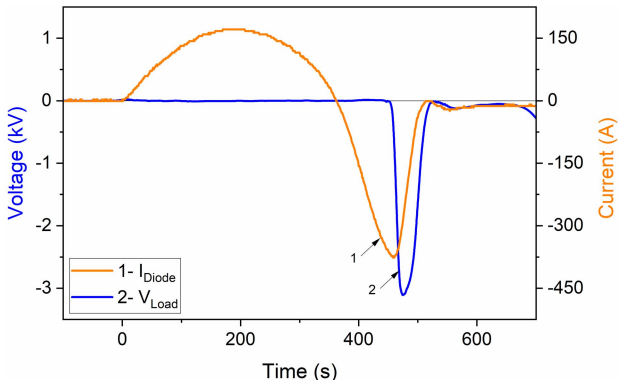

Fig. 5. Waveforms of 1—current flowing through the 64 (8 series × 8 parallel) TVS diodes assembly and 2—voltage pulse across the 110 Ω load at $V_C1 = 1.9$ kV.

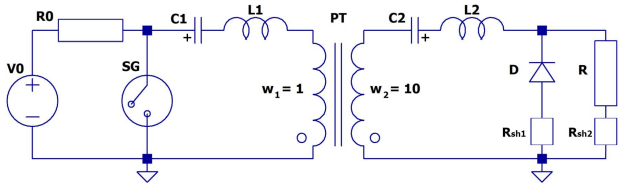

Fig. 6. Circuit diagram of the 10 J experimental arrangement. Explanations are provided in the text.

III. High-Energy 10 J Experimental Arrangement

A. Circuit Description

The equivalent electrical circuit of the high-energy test bench is presented in Fig. 6. This circuit is similar to the one presented in Fig. 1. A modification of the components was, however, implemented to increase the initially stored energy and, thereby, voltage amplitude across the load. Here, PT is based on a nanocrystalline magnetic core obtained from Finemet FT-3L, with the magnetic core parameters provided in [23]. The primary winding circuit consists of a film capacitor $C1 = 200$ nF, a triggered spark gap switch SG, and a single turn primary winding w_1. The secondary winding circuit consists of a ceramic capacitor $C2 = 2$ nF, a ten-turn secondary winding w_2, a diode D, and a resistive load R. To prevent any breakdown, the diode and the load are mounted under oil. Since the charging voltage of the primary capacitor is limited to 10 kV, the maximum initial electrostatic energy that can be stored is 10 J. The additional inductors $L1$ and $L2$ are further installed to vary the parameters of the forward and reverse pumping. The resetting circuit (not shown) consists of a five-turn bias winding driven by a dc current source with an amplitude up to 3 A. A choke (not shown) decouples the resetting circuit from the main circuit, preventing energy losses and protecting the current source. The operation of the circuit is similar to the one previously described in Section II.

The voltages V_C1 and V_C2 are measured using Tektronix P6015A and Northstar PVM100 probes, respectively. The waveforms are recorded by a DS1204B Rigol oscilloscope. The currents through the diode and the load are measured by two homemade resistive shunts (0.5 and 0.15 Ω) with a usable rise time of about 0.5 ns. The voltage across the load is found using Ohm's law. A 7 GHz Tektronix TDS7704B oscilloscope is used to capture the extremely fast signals generated by the diode and the load circuits. Wide bandwidth attenuators by Barth (26 dB, 30 GHz) and RF-Lambda (6 and 20 dB, 4 GHz) are used to attenuate the high-voltage signals obtained from resistive shunts.

B. High-Voltage Diodes

Several elementary off-the-shelf rectifier diodes were connected in series to build a high-voltage diode assembly having

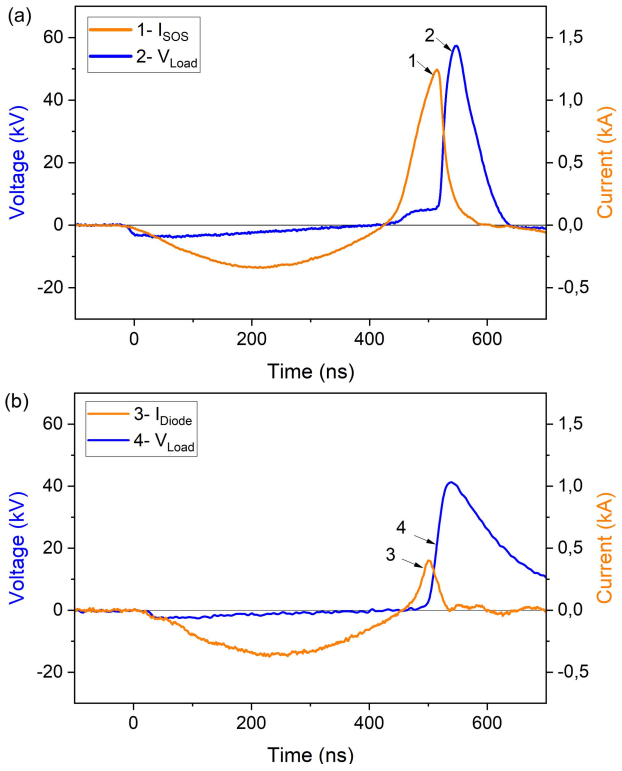

Fig. 7. Waveforms of the current through the diode D (1, 3) and voltage across the load $R = 70\ \Omega$ (2, 4) at $V_C1 = 6$ kV for (a) SOS-180-4 and (b) OTS-100.

an overall blocking voltage of about 100 kV. This diode is termed OTS-100. The characteristics obtained for OTS-100 on the 10 J test bench are compared with those of the SOS-180-4 diode [19], rated for 180 kV which serves as a reference.

C. Results and Discussion

First, the SOS-180-4 diode was tested on the 10 J test bench. The charging voltage of $C1$ (see Fig. 6) was fixed at 6 kV. A tubular non-inductive ceramic resistor $R = 70\ \Omega$ was used as a load. For the SOS-180-4 diode, the following parameters were obtained [see Fig. 7(a)]: forward pumping current $I^+ = 400$ A, duration $t^+ = 440$ ns, reverse pumping current $I^- = 1.3$ kA, and reverse pumping time $t^- = 90$ ns, while the cutoff time t_0 is 32 ns. The voltage pulse generated on the resistive load has an amplitude of 58 kV with a rise time of 19 ns, and a pulse duration of 55 ns (FWHM). The overvoltage coefficient K_{ov} of the SOS-180-4 diode is 1.2.

Second, the current and voltage pulse parameters obtained using OTS-100 operated under the same condition as SOS-180-4 are as follows [see Fig. 7(b)]: forward pumping current $I^+ = 370$ A, duration $t^+ = 440$ ns, reverse pumping current $I^- = 0.4$ kA, and reverse pumping time $t^- = 45$ ns. The cutoff time t_0 was 23 ns. The load voltage pulse has an amplitude of 42 kV, rise time of 22 ns, and pulse duration of 108 ns (FWHM). The overvoltage coefficient of OTS-100 is $K_{ov} = 0.85$.

Both SOS-180-4 and OTS-100 have practically the same forward pumping parameters I^+, t^+ and voltage drop

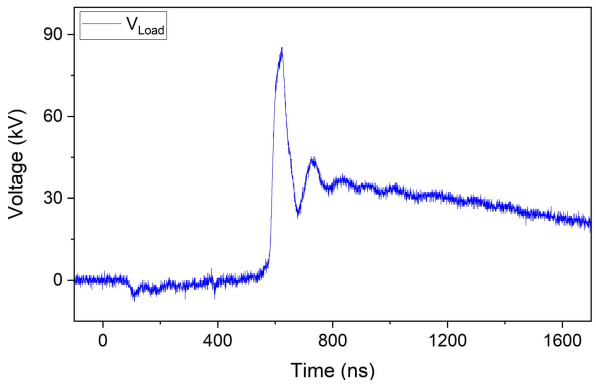

Fig. 8. Waveform of the voltage across load $R = 1$ kΩ at $V_C1 = 6$ kV.

(see Fig. 7). However, the behavior of OTS-100 during reverse pumping is changing dramatically: its reverse pumping time t^- is two times less when compared with the SOS-180-4 diode. Eventually, this leads to the threefold decrease in the reverse current I^-, which prevents storing energy in IES ($L2$ and parasitic inductance). While the reverse-to-forward-current ratio (I^-/I^+) of SOS-180-4 is 3.2, this ratio is only 1.1 for OTS-100. Hence, in the latter case, one part of the energy still remains stored in $C2$ at the current cutoff phase. Then both parts of the energy are switched into the load. As a consequence, the voltage pulse across the load has two clearly distinguished stages (see Fig. 8). The first high-voltage stage could be driven by the energy stored in the inductance $L2$; the second low-voltage stage could be driven by the discharge of the remaining energy in $C2$. Since the time constant of the capacitor discharge is increasing, this effect is accentuated for high-impedance loads. For example, for a 1 kΩ load, the complete discharge of the capacitor into the load occurs after a few μs (see Fig. 8).

D. Optimization of the OTS-100 Operating Mode

This section is dedicated to an examination of the main factors affecting the reverse pumping parameters of OTS-100 when operating as an opening switch. An experimental study was undertaken to find ways to increase the reverse pumping time, the inductive stored energy, and, therefore, all the output pulse parameters.

First, amplitude and duration of the forward and reverse pumping currents were varied, by changing V_C1 (see Fig. 6) from 3 to 10 kV. During these tests, by changing V_C1 and simultaneously adjusting the bias current, the voltage V_R across the 70 Ω load was adjusted almost linearly from 10 to 70 kV [see Fig. 9(a)]. This demonstrates a possibility of building an adjustable pulse power generator based on an opening switch combined with a saturating PT.

The maximum output voltage $V_R = 70$ kV with a rise time of 23 ns and duration of 100 ns (FWHM) was obtained for a 70 Ω load and for a charging voltage $V_C1 = 10$ kV, which corresponds to 10 J energy stored in $C1$ [see Fig. 9(a)]. The corresponding forward and reverse currents through the OTS-100 diode are $I^+ = 0.6$ kA and $I^- = 0.8$ kA, respectively. The

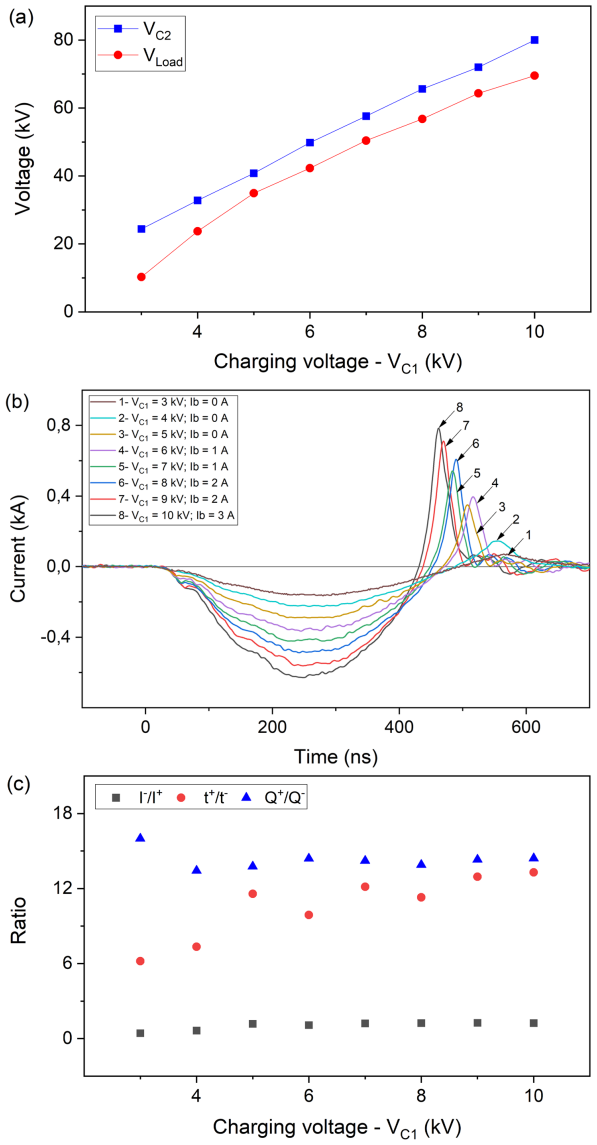

Fig. 9. Evolution of (a) voltages across $C2$ (square) and load (round); (b) current through the diode; and (c) ratios of the pumping currents (square), pumping times (round), and electric charges (triangle) as a function of the charging voltage V_C1 and time, using the OTS-100 diode and the resistive load $R = 70\ \Omega$.

load current reaches 1 kA, resulting in a load peak power of 70 MW.

The influence of V_C1 on diode pumping is presented in Fig. 9(b) and (c). When V_C1 increases, both I^+ and I^- increase, respectively, from 160 to 650 A, and from 70 to 800 A. At the same time, t^+ slightly decreases from 480 to 400 ns, while t^- decreases from 80 to 30 ns. Consequently, the ratio of the forward to reverse current duration t^+/t^- also increases. In addition, the ratio I^-/I^+ increases from 0.4 to 1.3 without approaching the SOS-180-4 diode current ratio of 3.2. It is worth mentioning a constant ratio of the forward and reverse electric charges Q^+/Q^- calculated as $Q = \int i(t)dt$ during diode forward and reverse pumping. For this experiment, the bias current [Ib in Fig. 9(b)] was fixed at zero for V_C1 from 3 to 5 kV; at 1 A for V_C1 from 6 to 7 kV; at 2 A for V_C1 from 8 to 9 kV; and 3 A for $V_C1 = 10$ kV.

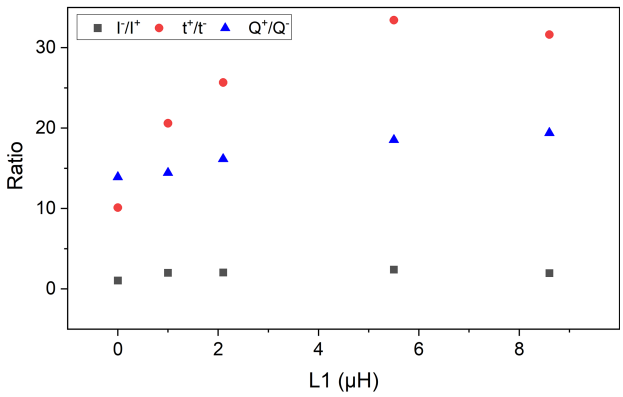

Fig. 10. Ratios of the pumping currents (square), pumping times (round), and electric charges (triangle) as a function of the inductance $L1$ obtained for OTS-100 at the resistive load $R = 50\ \Omega$ and charging voltage $V_C1 = 6$ kV.

To examine the impact of I^- magnitude on OTS-100 switching, an additional inductance $L1$ has been added in series with the capacitor $C1$, shown in Fig. 6. Fig. 10 summarizes the results. The inductance $L1$ was varied from 0 to 8.6 μH, causing the variation in I^- from 0.4 to 0.1 kA. During these experiments, I^+ and t^+ were changing as well, while t^- remained constant. For this experiment, a 50 Ω TVO less inductive resistor load is used. The charging voltage V_C1 was fixed at 6 kV. It was noted that increasing $L1$ causes the forward current duration to increase and the forward and reverse current amplitudes to decrease, while the reverse current duration remains about the same. This results in an increase in the ratio I^-/I^+ to 2.4. The t^+/t^- ratio obviously increases, as well as the forward to reverse electric charges.

High values of inductance $L1$ leads to a decrease in the maximum voltage at $C2$ and, therefore, lower voltage across the load. Although the current ratio I^-/I^+ is improved by adding $L1$, the load current and voltage amplitudes drop, and thus the use of a less inductive primary circuit is recommended.

According to [3], a nanosecond current cutoff in semiconductor diodes with a switching power from MW to GW can be realized using the drift step recovery diode (DSRD) or SOS. However, it seems that the results obtained in this work cannot be fully explained by these two mechanisms. While the limit of DSRD is 200–300 A/cm^2 [3], in the present work the OTS-100 diode operates at a current density of more than 1 kA/cm^2, which is usually considered as a threshold of the SOS mode [7]. Also, even though OTS-100 was tested at forward pumping mode required to the SOS mechanism, reverse pumping mode parameters were dramatically different from those expected from an SOS diode.

In particular, reverse pumping time t^-, which was limited by the reverse conductivity of the diode, was two times less compared with the SOS-180-4 diode. What is more important, t^- is almost insensitive to the forward pumping parameters such as t^+ and I^+. However, the cutoff time of the OTS-100 diode (tens of nanoseconds) is close to an SOS diode cutoff time at comparable voltage and power levels on the load. These facts probably require another mechanism of current interruption

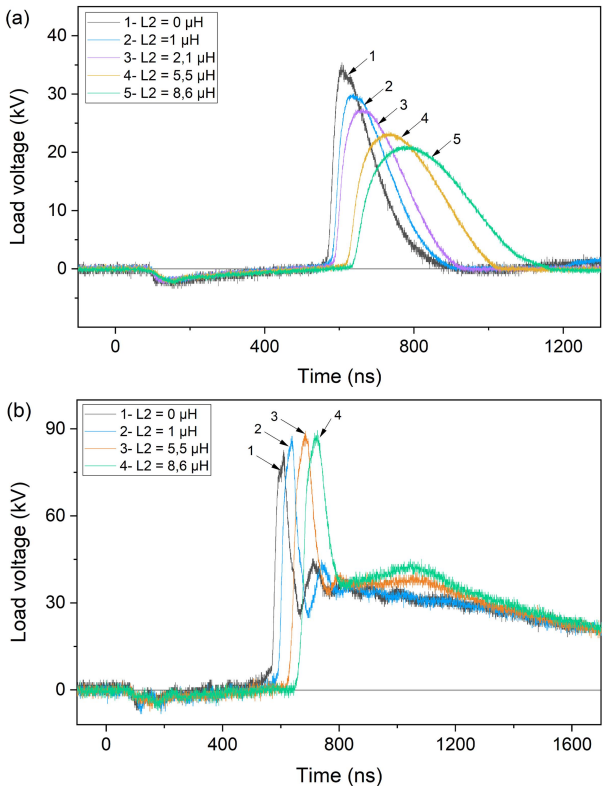

Fig. 11. Load voltage at different $L2$ on (a) 50 Ω load and (b) 1 kΩ load using the OTS-100 diode at charging voltage $V_C1 = 6$ kV.

TABLE II

LOAD VOLTAGE AMPLITUDE, RISE TIME, WIDTH, AND ENERGY EFFICIENCY AT DIFFERENT $L2$ ON 50 Ω AND 1 kΩ ($\eta = E_R/E_{C1}$)

R (Ω)	$L2$ (µH)	V_R (kV)	T_r (ns)	$FWHM$ (ns)	η (%)
50	0	35	23	116	58
	0.3	32	26	130	55
	1.0	30	29	150	56
	5.5	24	53	250	55
	8.6	21	71	290	55
1000	0	83	21	63	44
	0.3	84	24	64	43
	1.0	86	28	65	42
	5.5	88	33	85	46
	8.6	87	34	105	48

to be considered. At this moment, it is assumed that specific diode structure—engineered for a fast recovery—could be a reason for the fast current cutoff. However, to shed light on this question, one needs to know the exact doping profile of the diode, which is usually a trade secret of the manufacturer.

Finally, the inductance $L2$ (see Fig. 6) was installed to investigate its impact on the shape of the output voltage and on the energy transferred to the load. An experiment was performed on 50 Ω and 1 kΩ loads with $L1 = 0$. The results are presented in Fig. 11(a) and (b); and Table II summarizes the parameters of the output voltage pulse and the energy efficiency as a function of the inductance $L2$. The energy delivered into the load is numerically estimated as the integral of the load power. The stored energy in the capacitor is calculated as the half product of the capacitance and the square of the voltage ($E_{C1} = C_1 U_{C1}^2/2$).

As shown in Fig. 11(a) for the low-impedance load, the inductance $L2$ reduces the amplitude of the load voltage pulse and increases the pulse duration. The rise time is also extended and the input to output energy efficiency is not improved (see Table II). On the contrary, for high-impedance loads [see Fig. 11(b)], $L2$ improves in the first instance the high-voltage part of the voltage pulse. The amplitude and duration of the high-voltage part are probably increased due to an increase in the energy stored in $L2$, which changes from 80 to 260 mJ for $L2$ equal to 1 and 8.6 μH, respectively. In addition, the energy efficiency is slightly improved, though the rise time is increased (see Table II).

IV. CONCLUSION

The use of off-the-shelf diodes as SOSs has been investigated. Among the 25 off-the-shelf diodes tested with the low-energy test bench, the TVS diodes showed the best results in terms of switching time. The switching power of off-the-shelf diodes was increased by series–parallel connection. The series connection of off-the-shelf diodes increased the voltage capability of the switch, whereas parallel connection reduced its energy losses. It was shown that the output voltage can be linearly adjustable using a variable primary charging voltage combined with an appropriate resetting current. To optimize the energy efficiency of the circuit, the inductance of the primary circuit of the transformer should be minimized, while an appropriate secondary inductance should be determined depending on the load. The off-the-shelf diodes have shown a good stability in voltage switching after a large number of shots, with no degradation of the diodes being observed during experimentation. When combined with a solid-state primary switch and the implementation of an efficient cooling, the off-the-shelf diode assemblies represent a serious candidate to become a major asset in the development of high repetition rate nanosecond pulsed power systems.

REFERENCES

[1] H. Bluhm, *Pulsed Power Systems: Principles and Applications*. Berlin, Germany: Springer, 2006.
[2] S. N. Rukin, "Pulsed power technology based on semiconductor opening switches: A review," *Rev. Sci. Instrum.*, vol. 91, no. 1, Jan. 2020, Art. no. 011501.
[3] I. V. Grekhov and G. A. Mesyats, "Nanosecond semiconductor diodes for pulsed power switching," *Phys.-Uspekhi*, vol. 48, no. 7, pp. 703–712, Jul. 2005.
[4] S. Scharnholz, V. Brommer, G. Buderer, and E. Spahn, "High-power MOSFETs and fast-switching thyristors utilized as opening switches for inductive storage systems," *IEEE Trans. Magn.*, vol. 39, no. 1, pp. 437–441, Jan. 2003.
[5] W. Jiang *et al.*, "Compact solid-state switched pulsed power and its applications," *Proc. IEEE*, vol. 92, no. 7, pp. 1180–1195, 2004.
[6] I. V. Grekhov and G. A. Mesyats, "Physical basis for high-power semiconductor nanosecond opening switches," *IEEE Trans. Plasma Sci.*, vol. 28, no. 5, pp. 1540–1544, Oct. 2000.
[7] G. A. Mesyats *et al.*, "Semiconductor opening switch research at IEP," in *Proc. 10th IEEE Int. Pulsed Power Conf.*, Albuquerque, NM, USA, Jul. 1995, pp. 298–305.

[8] S. A. Darznek, G. A. Mesyats, S. N. Rukin, and S. N. Tsyranov, "Theoretical model of the SOS effect," in *Proc. 11th Int. Conf. High Power Beams*, Prague, Czech Republic, Jun. 1996, pp. 1241–1244.
[9] S. N. Rukin, "High-power nanosecond pulse generators based on semiconductor opening switches," *Instrum. Exp. Techn.*, vol. 42, no. 4, pp. 439–467, 1999.
[10] G. Wang, J. Su, Z. Ding, X. Yuan, and Y. Pan, "A semiconductor opening switch based generator with pulse repetitive frequency of 4 MHz," *Rev. Sci. Instrum.*, vol. 84, no. 12, pp. 9–12, 2013.
[11] S. K. Lyubutin *et al.*, "High efficiency nanosecond generator based on semiconductor opening switch," *IEEE Trans. Dielectr. Electr. Insul.*, vol. 18, no. 4, pp. 1221–1227, Aug. 2011.
[12] S. Y. Sokovnin and M. E. Balezin, "Improving the operating characteristics of an *Y*PT-0.5 accelerator," *Instrum. Experim. Techn.*, vol. 48, no. 3, pp. 392–396, May 2005.
[13] S. Y. Sokovnin and M. E. Balezin, "Repetitive nanosecond electron accelerators type URT-1 for radiation technology," *Radiat. Phys. Chem.*, vol. 144, pp. 265–270, Mar. 2018.
[14] T. Tang, F. Wang, A. Kuthi, and M. A. Gundersen, "Diode opening switch based nanosecond high voltage pulse generators for biological and medical applications," *IEEE Trans. Dielectr. Electr. Insul.*, vol. 14, no. 4, pp. 878–883, Aug. 2007.
[15] T. Sugai, W. Liu, A. Tokuchi, W. Jiang, and Y. Minamitani, "Influence of a circuit parameter for plasma water treatment by an inductive energy storage circuit using semiconductor opening switch," *IEEE Trans. Plasma Sci.*, vol. 41, no. 4, pp. 967–974, Apr. 2013.
[16] T. Sugai, W. Jiang, and A. Tokuchi, "Influence of forward pumping current on current interruption by semiconductor opening switch," *IEEE Trans. Dielectr. Electr. Insul.*, vol. 22, no. 4, pp. 1971–1975, Aug. 2015.
[17] A. S. Kesar *et al.*, "A fast avalanche Si diode with a 517 μm low-doped region," *Appl. Phys. Lett.*, vol. 117, no. 1, Jul. 2020, Art. no. 013501.
[18] K. Takaki, I. Yagi, S. Mukaigawa, T. Fujiwara, and T. Go, "Ozone synthesis using streamer discharge produced by nanoseconds pulse voltage under atmospheric pressure," in *Proc. IEEE Pulsed Power Conf.*, Jun. 2009, pp. 989–993.
[19] A. I. Gusev, S. K. Lyubutin, A. V. Ponomarev, S. N. Rukin, and B. G. Slovikovsky, "Semiconductor opening switch generator with a primary thyristor switch triggered in impact-ionization wave mode," *Rev. Sci. Instrum.*, vol. 89, no. 11, Nov. 2018, Art. no. 114702.
[20] Vacuumschmelze. *Nanocrystalline Material*. Accessed: May 2020. [Online]. Available: https://www.vacuumschmelze.com/Nanocrystalline-Material
[21] J.-G. Choi, "Introduction of the magnetic pulse compressor (MPC)—Fundamental review and practical application," *J. Electr. Eng. Technol.*, vol. 5, no. 3, pp. 484–492, Sep. 2010.
[22] A. V. Ponomarev, S. N. Rukin, and S. N. Tsyranov, "Investigation of the process of voltage distribution over elements of a high-power semiconductor current interrupter," *Tech. Phys. Lett.*, vol. 27, no. 10, pp. 857–859, Oct. 2001.
[23] J. Holma and M. J. Barnes, "Prototype inductive adders with extremely flat-top output pulses for the compact linear collider at CERN," *IEEE Trans. Plasma Sci.*, vol. 46, no. 10, pp. 3348–3358, Oct. 2018.

Mawuena Rémi Degnon (Graduate Student Member, IEEE) was born in Lomé, Togo, in 1996. He received the M.Eng. degree in electrical engineering from the Université de Lomé, Lomé, in 2018, and the M.Sc. degree in electrical engineering and industrial computing from the Université de Pau et des Pays de l'Adour (UPPA), Pau, France, in 2020, where he is currently pursuing the Ph.D. degree with the Laboratoire des Sciences de l'Ingénieur Appliquées à la Mécanique et au Génie Électrique (SIAME Laboratory).

His research interests include high-voltage pulsed power systems, solid-state switches, and nanosecond high-voltage generators for industrial applications.

Anton I. Gusev (Member, IEEE) was born in Miass, Russia, in 1988. He received the M.S. degree in electrophysics from Ural Federal University (UrFU), Yekaterinburg, Russia, in 2012, and the Ph.D. degree in engineering sciences from the Institute of Electrophysics, Ural Branch of the Russian Academy of Sciences (IEP), Yekaterinburg, in 2019.

From 2008 to 2019, he was with IEP as an Intern, a Ph.D. Student, and a Junior Researcher with the Pulsed Power Laboratory. At the same time, from 2014 to 2019, he was with UrFU as a Senior Teacher. In 2019, he became a Post-Doctoral Researcher with the Université de Pau et des Pays de l'Adour (UPPA), Pau, France, where he has been an Assistant Professor with the Laboratoire des Sciences de l'Ingénieur Appliquées à la Mécanique et au Génie Électrique (SIAME Laboratory) since 2020. His research interests include semiconductor physics, high-power semiconductor switches, and high-voltage solid-state generators, which provide nano- and subnanosecond pulses.

Dr. Gusev is a member of the International Society on Pulsed Power Applications (ISP) and the Association for the Advancement of Pulsed Power (A2P2). He has been awarded the Young Researcher at major international pulsed power conferences (the Energy Fluxes and Radiation Effects (EFRE) 2016, the Euro-Asian Pulsed Power Conference (EAPPC) 2018, and the Gas Discharge Plasmas and Their Applications (GDP) 2021), including two supported by IEEE Pulsed Power Conference (PPC) 2017 and the IEEE International Power Modulator and High Voltage Conference (IPMHVC) 2018.

Antoine Silvestre de Ferron was born in Tarbes, France, in 1977. He received the master's degree in electrical and electronic engineering from the University of Toulouse, Toulouse, France, in 2002, and the Ph.D. degree in electrical engineering from the Université de Pau et des Pays de l'Adour (UPPA), Pau, France, in 2006.

From 2006 to 2008, he was a Researcher with the Atomic Energy Commission (CEA), Le Barp, France, a French government-fund technological research organization. He is currently an Engineer with the Head of the High-Voltage Processes Team, Laboratoire des Sciences de l'Ingénieur Appliquées à la Mécanique et au Génie Électrique (SIAME Laboratory), UPPA. His research interest includes high pulsed power generation with military and civil applications. He is specialized in Marx generator and pulse forming lines in high-voltage generation, high-voltage transient probes associated, and high-current discharges in liquids.

Laurent Pécastaing (Senior Member, IEEE) received the Ph.D. and Research Directorship Habilitation degrees in electrical engineering from the Université de Pau et des Pays de l'Adour (UPPA), Pau, France, in 2001 and 2010, respectively.

He is currently a Full Professor in pulsed power with UPPA. He is also the Director of the Laboratoire des Sciences de l'Ingénieur Appliquées à la Mécanique et au Génie Électrique (SIAME Laboratory) and a common laboratory between UPPA and the Atomic Energy Commission (CEA), Le Barp, France. His current research interests include high-power microwave sources, compact pulsed power systems, and ultrafast transient probes.

Dr. Pécastaing is a member of the International Steering Committees for the BEAMS Conference and the Euro-Asian Pulsed Power Conference. He was the Chairperson of the Euro-Asian Pulsed Power Conference (EAPPC)/High-Power Particle Beams (BEAMS)/Megagauss Magnetic Field Generation and Related Topics (MEGAGAUSS) Conference in France, in 2021.

Gaëtan Daulhac was born in Brive la Gaillarde, France, in 1987. He received the M.Eng. degree from ENSIAME, Famars, France, in 2010, and the research master's degree from the Université de Valencienne (UVHC), Valenciennes, France, in 2010.

He is currently an Engineer with ITHPP ALCEN, Thégra, France. He works on high pulsed power generator, more precisely on resonant generator, dedicated to pulse electron beams sterilization.

Aleksandr Baranov received the M.Eng. degree in industrial electrical energy and engineering from Togliatti State University, Togliatti, Russia, in 2015.

He is currently a Research and Development Engineer with ITHPP ALCEN, Thégra, France. His research fields of interests are high-voltage nanoseconds 'generators, electron emission, and pulsed power systems.

Sébastien Boisne was born in Thionville, France, in 1979. He received the master's degree in global management of organizations, strategy, and finance from the University of Paris Dauphine PSL, Paris, France, in 2016.

In 2002, he joined Thomson CSF Linac, Orsay, France, a Leader in linear electron accelerators, where he was in charge of the development of electron beam range of products, intended to be employed in high-demand industrial uses. He is currently with the Head of BETA BEAMS, ITHPP-ALCEN Group, Donzenac, France, specializing in the design and supply of electron beam accelerators, installed on end-users' production sites, and mainly used in surface and core sterilization of pharmaceutical products.

Bucur Mircea Novac (Senior Member, IEEE) received the M.Sc. and Ph.D. degrees from the University of Bucharest, Bucharest, Romania, in 1977 and 1989, respectively.

He joined Loughborough University, Loughborough, U.K., in 1998, where he is currently a Professor of pulsed power. He has coauthored two books on explosive pulsed power and has published more than 200 refereed articles and conference contributions. His research interests include compact and repetitive high-power systems, explosively and electromagnetically driven magnetic flux compression generators and their applications, electromagnetic launchers, ultrafast magneto and electrooptic sensors, and 2-D modeling of pulsed power systems.

Prof. Novac is a member of the International Steering Committees for the MEGAGAUSS Conference and the Euro-Asian Pulsed Power Conference (EAPPC). He is a fellow of the Royal Academy of Engineering, and a Chartered Engineer and a fellow of the Institution of Engineering and Technology, U.K. He was a Voting Member of the Pulsed Power Science and Technology Committee of the IEEE Nuclear and Plasma Science Society, a member of the Organizing Committee of the IEEE International Power Modulator and High Voltage Conference, and the Co-Chairperson of the U.K. Pulsed Power Symposia.